Article

Cell Reports

Cbx4 Sumoylates Prdm16 to Regulate Adipose Tissue Thermogenesis

Graphical Abstract

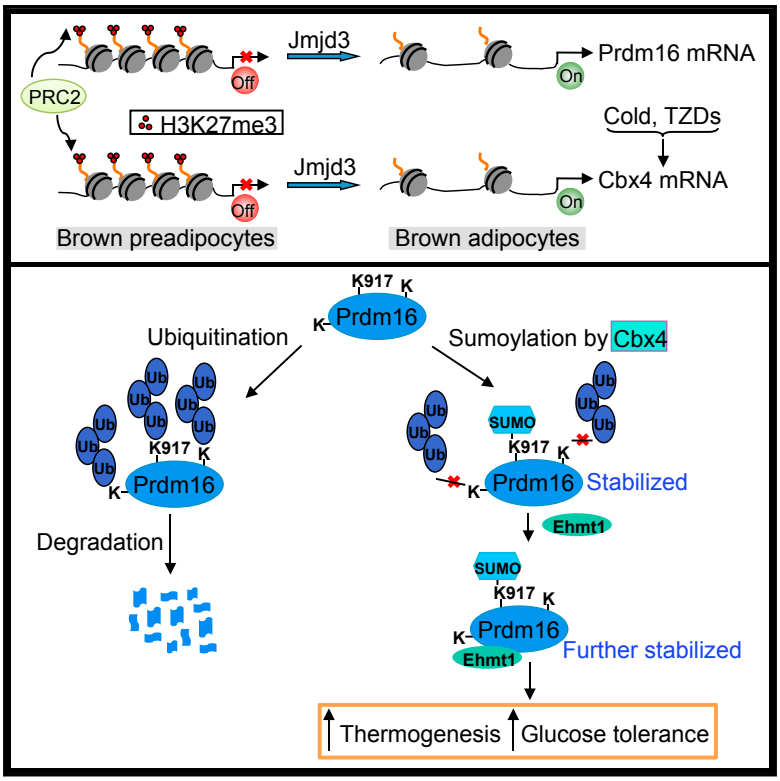

Highlights

- Cbx4 sumoylates thermogenic regulator Prdm16 at Lys 917
- Sumoylation of Prdm16 blocks its ubiquitination and, thus, augments its stability
- Sumoylation of Prdm16 primes Prdm16 to be further stabilized by Ehmt1
- Cbx4 regulates adipose tissue thermogenic function through sumoylating Prdm16

Authors

Qingbo Chen, Lei Huang, Dongning Pan, Lihua J. Zhu, Yong-Xu Wang

Correspondence

yongxu.wang@umassmed.edu

In Brief

Chen et al. show that sumoylation of a key thermogenic regulator, Prdm16, at lysine 917 by Cbx4 blocks its ubiquitination-mediated degradation and, consequently, augments its stability. Sumoylation of Prdm16 is also a prerequisite for Ehmt1-mediated stabilization. At least in part through sumoylating Prdm16, Cbx4 promotes adipose thermogenic function.

Chen et al., 2018, Cell Reports 22, 2860–2872
March 13, 2018
https://doi.org/10.1016/j.celrep.2018.02.057

OPEN ACCESS
CellPress

Cell Reports
Article

Cbx4 Sumoylates Prdm16 to Regulate Adipose Tissue Thermogenesis

Qingbo Chen,[1] Lei Huang,[1] Dongning Pan,[2] Lihua J. Zhu,[1] and Yong-Xu Wang[1,3,*]
[1]Department of Molecular, Cell and Cancer Biology and Program in Molecular Medicine, University of Massachusetts Medical School, Worcester, MA 01605, USA
[2]Key Laboratory of Metabolism and Molecular Medicine, Department of Biochemistry and Molecular Biology, Fudan University Shanghai Medical College, Shanghai 200032, China
[3]Lead Contact
*Correspondence: yongxu.wang@umassmed.edu
https://doi.org/10.1016/j.celrep.2018.02.057

SUMMARY

Transcriptional co-activator Prdm16 controls brown fat development and white fat browning, but how this thermogenic function is modulated post-translationally is poorly understood. Here, we report that Cbx4, a Polycomb group protein, is a SUMO E3 ligase for Prdm16 and that Cbx4-mediated sumoylation of Prdm16 is required for thermogenic gene expression. Cbx4 expression is enriched in brown fat and is induced in adipose tissue by acute cold exposure. Sumoylation of Prdm16 at lysine 917 by Cbx4 blocks its ubiquitination-mediated degradation, thereby augmenting its stability and thermogenic function. Moreover, this sumoylation event primes Prdm16 to be further stabilized by methyltransferase Ehmt1. Heterozygous Cbx4-knockout mice develop metabolic phenotypes resembling those of Prdm16-knockout mice. Furthermore, fat-specific Cbx4 knockdown and overexpression produce remarkable, opposite effects on white fat remodeling. Our results identify a modifying enzyme for Prdm16, and they demonstrate a central role of Cbx4 in the control of Prdm16 stability and white fat browning.

INTRODUCTION

Classical brown fat (brown adipose tissue [BAT]) and brown-like (beige) adipocytes are specialized to dissipate energy as heat through non-shivering thermogenesis (Cannon and Nedergaard, 2004; Harms and Seale, 2013; Kajimura et al., 2015; Rosen and Spiegelman, 2014). These adipocytes express a unique set of BAT-selective genes, including mitochondrial inner membrane protein Uncoupling protein 1 (Ucp1), a key thermogenic effector for heat production. While classical BAT adipocytes, present at discrete anatomical regions, are generated during embryogenesis, beige adipocytes are formed postnatally within white fat tissues (white adipose tissue [WAT]) in response to external cues, a process often called browning (Giordano et al., 2014; Kajimura et al., 2015). Studies in recent years suggest that adult humans possess both classical BAT and beige adipocytes that are highly inducible and are inverse-associated with body weight index (Chen et al., 2016), underscoring their potential as therapeutic targets for obesity and metabolic diseases.

Although arising from distinct developmental origins (Kajimura et al., 2015), classic BAT and beige adipocytes share, to a great extent, common molecular mechanisms to control a BAT-selective gene program and thermogenic function (Harms and Seale, 2013; Kajimura et al., 2015). Among them, transcriptional control by co-activator Prdm16 is a predominant mechanism (Cohen et al., 2014; Harms et al., 2014; Seale et al., 2007, 2011). Emerging evidence indicates that Prdm16 is tightly regulated post-translationally. Prdm16 is a short-lived protein, and, upon ubiquitination by an unknown E3 ligase, it is rapidly degraded by the 26S proteasome pathway (Ohno et al., 2012). Remarkably, Prdm16 protein is stabilized by ectopic expression of methyltransferase Ehmt1 (Ohno et al., 2013) and by treatment of adipocytes with PPARγ full agonists, such as rosiglitazone (Ohno et al., 2012). These studies shed important light on how the proteasome-mediated Prdm16 degradation is counterbalanced; however, the underlying mechanism remains to be elucidated. Moreover, except for ubiquitination, other forms of potential post-translational modifications of Prdm16 have not been characterized, and no modifying enzyme has been identified.

Polycomb group (PcG) proteins are major epigenetic regulators of gene silencing that play crucial roles in cell lineage commitment, cell proliferation and differentiation, senescence, and cancer (Bracken and Helin, 2009; Sparmann and van Lohuizen, 2006; Surface et al., 2010). PcG proteins form two distinct protein complexes known as Polycomb-repressive complex 1 (PRC1) and PRC2. PRC2 contains Ezh2, Eed, and Suz12 and catalyzes trimethylation of histone H3 lysine 27 (H3K27me3). Canonical PRC1 is formed by four different orthologs, and each is a representative of Cbx, Pcgf, Hph, and ubiquitin E3 ligase Ring proteins. The two complexes can act either in concert (Simon and Kingston, 2009) or independently of each other (Boyer et al., 2006; Ku et al., 2008; Leeb et al., 2010) to repress gene expression. In addition, PRC1 has been implicated in transcriptional activation (Creppe et al., 2014; Frangini et al., 2013) as well as complex-independent function (Luis et al., 2011; Tan et al., 2011). Notably, among the five Cbx members (Cbx2, 4,

6, 7, and 8), Cbx4 is the only protein that possesses SUMO E3 ligase activity (Kagey et al., 2003).

We have previously shown that PRC2-catalyzed H3K27me3 modification prepares and safeguards a BAT-selective gene expression program in BAT development and browning of WAT (Pan et al., 2015). To date, it is unknown whether PRC1 or any of its subunits plays a role in adipose development and function. In this paper, we identify Cbx4 as a SUMO E3 ligase for Prdm16, and we reveal an unexpected post-translational regulatory mechanism underlying adipose thermogenesis.

RESULTS

Cbx4 Gene Is Marked by H3K27me3 in Brown Preadipocytes and Is Selectively Expressed in BAT

A significant subset of BAT-selective genes, including key thermogenic transcriptional regulators such as Prdm16, Pparα, and Pgc1β, was marked by H3K27me3 at their promoter/enhancer regions in brown preadipocytes (Pan et al., 2015). We surmised that potential thermogenic regulators might possess a similar pattern of H3K27me3 modification and gene expression. We therefore analyzed published chromatin immunoprecipitation sequencing (ChIP-seq) (GEO: GSE55469) and RNA sequencing (RNA-seq) (GEO: GSE56367) datasets (Pan et al., 2015), and we identified Cbx4 as a candidate. As shown in Figure 1A, Cbx4 promoter was modified by H3K27me3 in brown preadipcoytes, and this modification was largely removed in mature brown adipocytes. Cbx4 mRNA expression was significantly higher in BAT compared to epididymal WAT (10.6 versus 2.9 fragments per kilobase per million mapped reads [FPKMs]), which was confirmed by qRT-PCR and western blot analyses (Figure 1B). Cbx4 expression increased during brown adipocyte differentiation (Figure 1C). Moreover, we observed an induction of Cbx4 expression in BAT and subcutaneous inguinal WAT (iWAT) by acute cold exposure (Figure 1D) and in iWAT by β3 adrenergic receptor agonist (Figure 1E) and a decreased Cbx4 expression in the BAT of *ob/ob* mice (Figure 1F). These data indicate a potential role of Cbx4 in thermogenesis.

Cbx4 Stabilizes Prdm16 Protein

To identify the function of Cbx4 in adipocytes, we infected immortalized brown adipocytes at differentiation day 4 with Cbx4-knockdown adenovirus, and we collected samples at day 6. Knockdown of Cbx4 had no effects on general adipogenesis, as indicated by oil red O staining and the expression of the common fat marker aP2, but it significantly downregulated the expression of BAT-selective genes Ucp1 and Cidea (Figure 2A). Given the important role of Prdm16 in thermogenic gene expression, we examined its expression. Unexpectedly, while Prdm16 mRNA level was not affected (Figure 2A), its protein level was strongly decreased, whereas levels of Pgc1α and PPARδ were unchanged (Figure 2B). These results raise the possibility that Cbx4 might regulate Prdm16 protein stability. To test this possibility, we expressed Prdm16 and Cbx4 plasmids in HEK293 cells, and we observed that Cbx4 indeed augmented protein level of Prdm16 without affecting its mRNA level (Figure 2C). As a control, Cbx4 had no effect on Pgc1α protein level. To determine whether this increased protein accumulation of Prdm16 was due to slower protein degradation, we performed a cycloheximide chase assay. We found that Cbx4 expression extended the half-life time of Prdm16 protein from 8.5 to 14.3 hr (Figure 2D). Interestingly, the stabilization of Prdm16 by Cbx4 was not further enhanced by co-treatment of the cells with the 26S proteasome inhibitor MG132 (Figure 2E). These data suggest that Cbx4 stabilizes Prdm16 by blocking 26S proteasome-mediated degradation, which likely accounts for Cbx4-induced thermogenic gene expression.

Cbx4 Is a SUMO E3 Ligase for Prdm16

Cbx4 contains two SUMO-interacting motifs (SIMs) and a chromodomain, responsible for its SUMO E3 ligase activity and H3K27me3-binding activity, respectively. To determine which domain is required for Prdm16 stabilization, we generated mutants harboring SIM deletions or double point mutations at chromodomain (F11A/W35L). The F11A/W35L mutant has been shown to lose its binding to H3K27me3 and, thus, its polycomb-dependent function (Li et al., 2014). The mutants were transfected along with Prdm16 plasmids into HEK293 cells. We found that Cbx4 with SIM1 deletion (ΔSIM1) was no longer able to stabilize Prdm16, while SIM2 and the chromodomain were dispensable (Figure 3A). We next tested whether Prdm16 interacts with wild-type or mutant Cbx4. In this experiment, the amounts of Prdm16 plasmids transfected were adjusted to obtain similar levels of Prdm16 protein expression in each sample. We found that wild-type Cbx4 associated with Prdm16, and, interestingly, this association was enhanced when SIM1 was deleted (Figure 3B), suggesting that their interaction is not sufficient to stabilize Prdm16. These data led to the idea that Cbx4 stabilizes Prdm16 through sumoylation. Indeed, ectopic expression of wild-type Cbx4 effectively sumoylated ectopically expressed Prdm16, while the ΔSIM1 mutant was inactive (Figure 3C).

Sumoylation can occur through several different modes (Gareau and Lima, 2010). Our results are consistent with an idea that one of the possible functions of the SIM domain is to recruit SUMO-loaded Ubc9 and deliver activated SUMO to its substrates, instead of directly involving interaction with substrates (Gareau and Lima, 2010). How does Cbx4-mediated sumoylation stabilize Prdm16? As sumoylation has been shown to prevent ubiquitination of its substrates (Johnson, 2004), we examined the status of ubiquitination of Prdm16. Consistent with what was reported previously (Ohno et al., 2012), Prdm16 was highly ubiquitinated (Figure 3D). Expression of wild-type Cbx4 completely blocked ubiquitination of Prdm16, and the sumoylation-defective mutant ΔSIM1 had no effect (Figure 3D). Of note, in both sumoylation and ubiquitination assays, we pretreated cells with the 26S proteasome inhibitor MG132 to bring the input of Prdm16 protein to similar levels, allowing us to compare the level of modified Prdm16. Our results together show that Cbx4 sumoylates Prdm16, which in turn prevents its ubiquitination-mediated degradation.

Cbx4 Sumoylates Prdm16 at Lysine 917

Many sumoylated Lys residues are located within a ψ-K-X-E/D consensus motif, where ψ is a large hydrophobic residue (Rodriguez et al., 2001). Examination of the primary amino acid

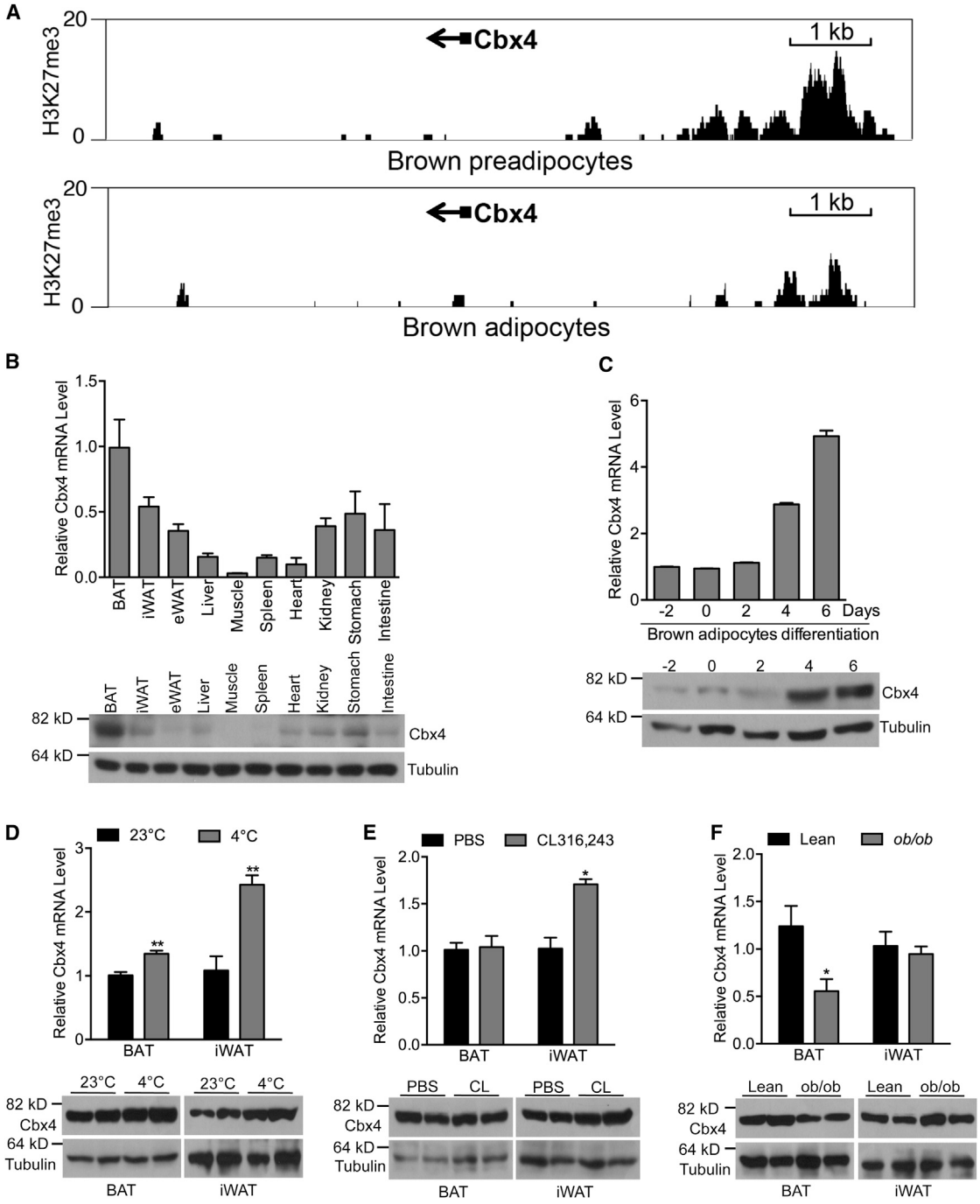

Figure 1. Cbx4 Is Enriched in BAT and Is Induced by Acute Cold Exposure

(A) H3K27me3 signal tracks are shown for Cbx4 loci in brown preadipocytes and mature adipocytes. Small black boxes and arrows depict the first exon and transcript orientation, respectively. Numbers at the top left of each graph represent the number of reads.

(B) Top: qPCR analysis of Cbx4 mRNA expression in multiple tissues from 12-week-old male mice (n = 4 mice). Data represent mean ± SEM. Bottom: western blot analysis of Cbx4 protein levels in different tissues is shown.

(C) Cbx4 mRNA (n = 3) and protein expression at different time points of *in vitro* differentiation of immortalized brown preadipocytes. Data represent mean ± SEM.

(D) Cbx4 mRNA (n = 4 mice/group) and protein expression in BAT and iWAT of 8-week-old male mice at 23°C or 4°C for 10 hr. Data represent mean ± SEM. $^{**}p < 0.01$.

(E) Cbx4 mRNA (n = 5 mice/group) and protein expression in BAT and iWAT of 8-week-old female mice intraperitoneally injected with PBS or 1 mg/kg CL316,243 for 2 days. Data represent mean ± SEM. $^{*}p < 0.05$.

(F) Cbx4 mRNA (n = 3–5 mice/group) and protein expression in BAT and iWAT of 3-month-old male ob/ob mice and lean mice. Data represent mean ± SEM. $^{*}p < 0.05$.

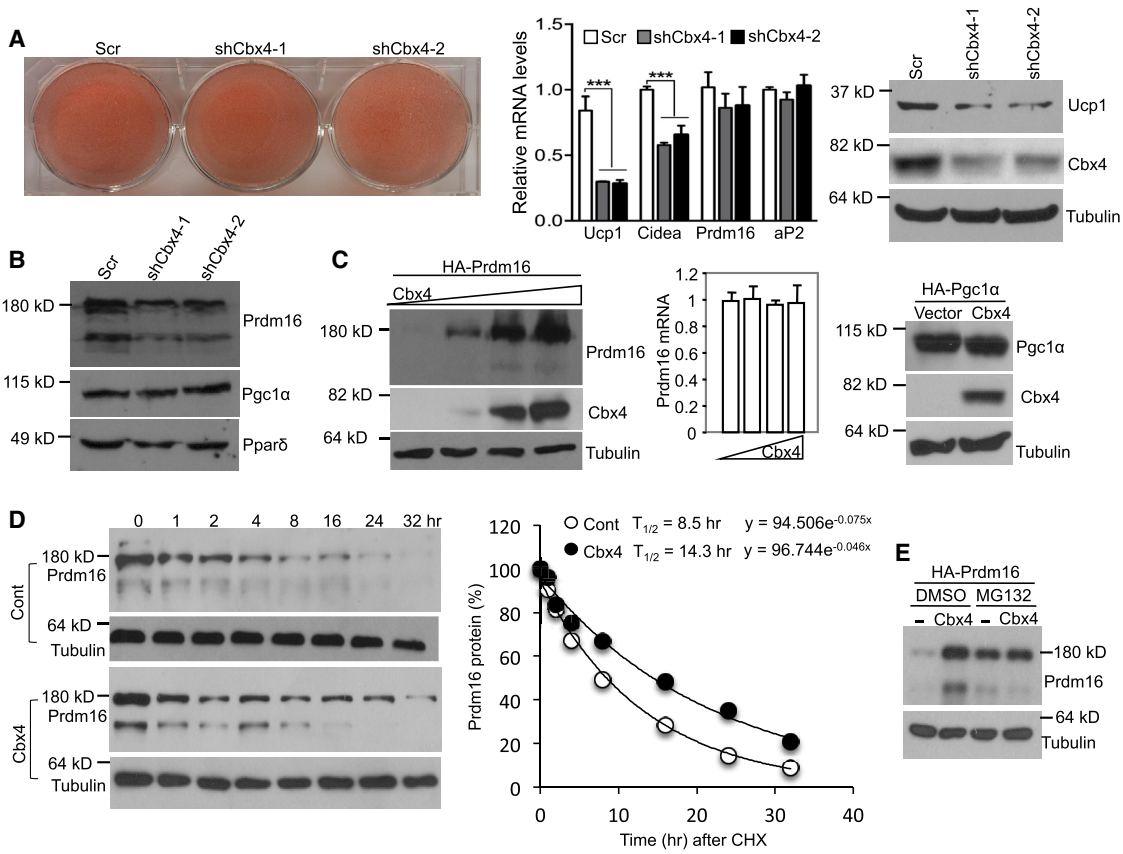

Figure 2. Cbx4 Stabilizes Prdm16

(A) Immortalized brown adipocytes were infected with Cbx4-knockdown adenoviruses during differentiation. The oil red O staining of triglycerides, qPCR analysis of gene expression (n = 4), and western blot analysis of Cbx4 and Ucp1 protein were performed. qPCR data represent mean ± SEM. ***p < 0.001, one-way ANOVA.

(B) Prdm16 protein level in brown adipocytes with Cbx4 knockdown.

(C) Prdm16 mRNA (n = 3) and protein expression in HEK293 cells co-transfected with Prdm16 and Cbx4 plasmids. Data represent mean ± SEM.

(D) HEK293 cells were co-transfected with Prdm16 and Cbx4 or vector plasmids and treated with cycloheximide (CHX). Prdm16 protein was examined at the indicated time points and quantified with ImageJ.

(E) HEK293 cells were co-transfected with Prdm16 and Cbx4 plasmids and then treated with MG132 or DMSO for 6 hr. Prdm16 protein level was examined.

sequence of murine Prdm16 revealed the presence of this consensus motif at K270, K754, and K917, which are also conserved in human Prdm16. Interestingly, K754 (equivalent to K752 in human Prdm16) was found to be sumoylated in HEK293 cells (Lamoliatte et al., 2014; Nishikata et al., 2011), although the identity of the corresponding E3 ligase was unknown. To determine whether any of the three Lys residues is sumoylated by Cbx4, Lys-to-Arg mutants of Prdm16 were generated. We found that stabilization of Prdm16 protein by Cbx4 overexpression largely disappeared in the K917R mutant, whereas K754R and K270R mutants remained fully stabilized (Figure 3E), raising the possibility that K917 might be a sumoylation site. Of note, in the absence of Cbx4 transfection, levels of wild-type Prdm16 and K754R and K270R mutants were also higher than that of the K917R mutant (Figure 3E, top panel), which was likely due to a very low but detectable endogenous Cbx4 protein expression (Figure 3E, middle panel). K917R mutant was still capable of interacting with Cbx4 (Figure S1), again indicating that their interaction is not sufficient to stabilize Prdm16. Importantly, K917R mutant showed a great, but not complete, loss of Cbx4-mediated sumoylation, whereas sumoylation of the K754R mutant by Cbx4 was indistinguishable from that of wild-type Prdm16 (Figure 3F). Consistent with these results, blockage of ubiquitination by Cbx4 was at least partially relieved in the K917 mutant compared with wild-type and K754R Prdm16 (Figure 3G). Our data collectively suggest that K917 of Prdm16 is a primary sumoylation site by Cbx4 and sumoylation of this site decreases ubiquitination on other Lys residues. On the other hand, K754 appears to be sumoylated by a different E3 ligase.

Cbx4 and Ehmt1 Act Synergistically to Stabilize Prdm16

Ehmt1 enhances Prdm16 stability through their direct interaction (Ohno et al., 2013). We explored whether Cbx4 and Ehmt1 work in concert to stabilize Prdm16. We confirmed previous finding that Prdm16 protein was stabilized by Ehmt1 through co-expression in Cos7 cells (Ohno et al., 2013) (Figure 3H). Surprisingly, this stabilization by Ehmt1 was abolished by the expression of

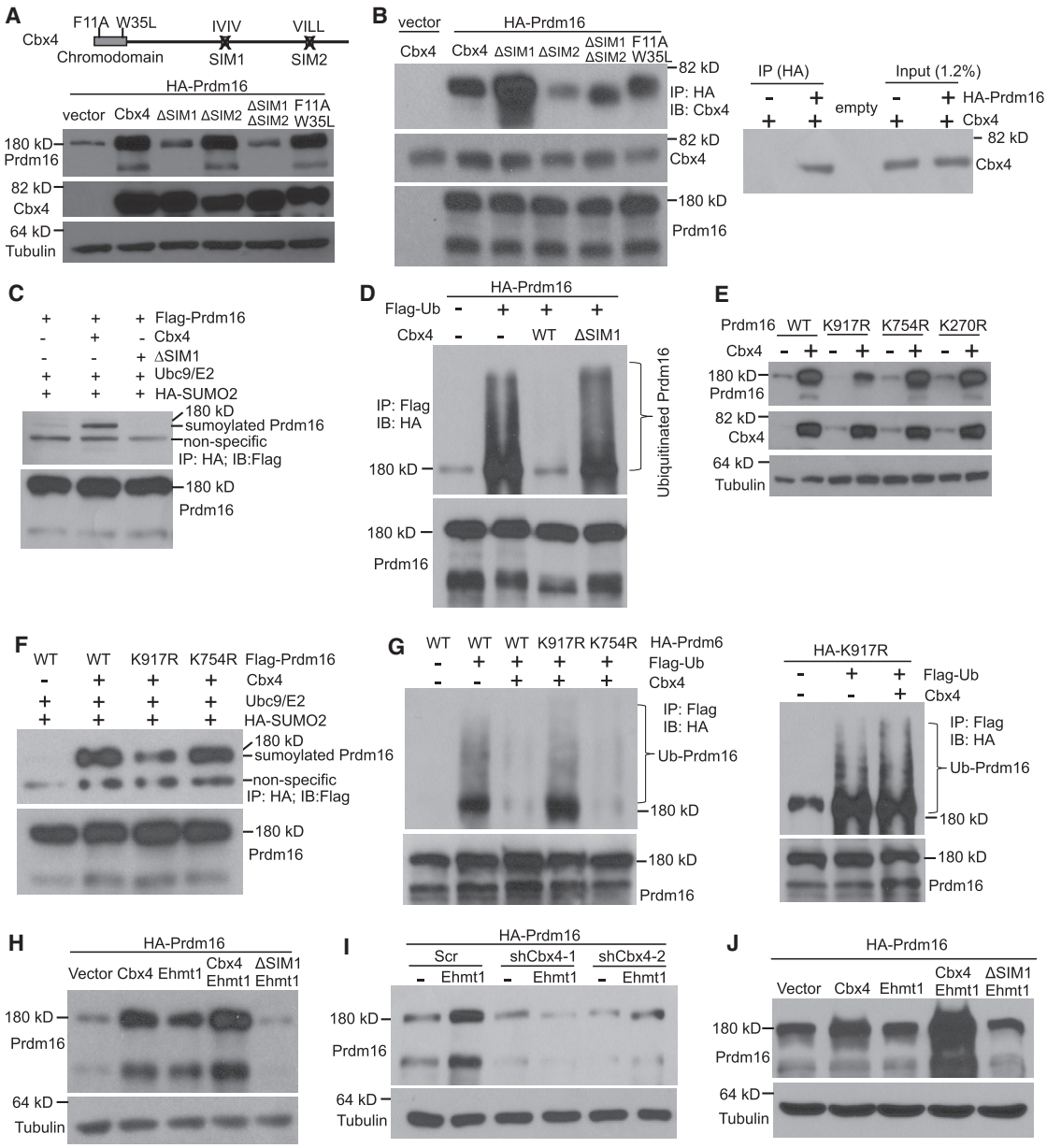

Figure 3. Cbx4 Sumoylates Prdm16 at Lys 917 to Inhibit Its Ubiquitination and to Prime Its Further Stabilization by Ehmt1

(A) Top panel depicts Cbx4 mutant constructs, and bottom panel shows Prdm16 protein level in HEK293 cells co-transfected with Prdm16 and Cbx4 mutant plasmids.

(B) Left: interaction of Prdm16 with Cbx4 in HEK293 cells co-transfected with the indicated plasmids. Right: level of Cbx4 present in the Prdm16 immunoprecipitates relative to total Cbx4 is shown.

(C) Sumoylation of Prdm16 was assayed in HEK293 cells co-transfected with the indicated plasmids.

(D) Ubiquitination of Prdm16 was assayed in HEK293 cells co-transfected with the indicated plasmids.

(E) HEK293 cells were co-transfected with wild-type or mutant Prdm16 plasmids along with vector or Cbx4 plasmids. Prdm16 protein level was examined.

(F) Sumoylation of wild-type or mutant Prdm16 was assayed in HEK293 cells co-transfected with the indicated plasmids.

(G) Ubiquitination of wild-type or mutant Prdm16 was assayed in HEK293 cells co-transfected with the indicated plasmids.

(H) Prdm16 protein levels in Cos7 cells co-transfected with the indicated plasmids.

(I) Cos7 cells were infected with Cbx4-knockdown lentivirus and then co-transfected with the indicated plasmids. Prdm16 protein was analyzed.

(J) Prdm16 protein level in HEK293 cells co-transfected with the indicated plasmids.

Cbx4 ΔSIM1 mutant (Figure 3H), suggesting a dominant-negative effect of this mutant over endogenous Cbx4. Indeed, Cos7 cells had a robust expression of endogenous Cbx4 protein that was about one-third of the level we typically obtained from HEK293 cells transfected with Cbx4 (Figure S2A). Importantly, lentiviral knockdown of Cbx4 in Cos7 cells blocked Ehmt1-mediated stabilization of Prdm16 (Figure 3I; Figure S2B), an effect similar to what was produced by ΔSIM1 expression (Figure 3H). Since Cbx4 did not sumoylate Ehmt1 and Ehmt1 did not enhance Cbx4 sumoylation activity for Prdm16 (Figure S3), our data indicate that sumoylation of Prdm16 by Cbx4 might prime Prdm16 for further stabilization by Ehmt1. To test this further, we performed co-transfection in HEK293 cells; these cells expressed extremely low endogenous Cbx4 protein compared with Cos7 cells (Figure S2A). In contrast to what occurred in Cos7 cells, expression of Ehmt1 alone was not able to stabilize Prdm16. However, in the presence of wild-type Cbx4, but not ΔSIM1 mutant, Ehmt1 strongly enhanced Prdm16 stability (Figure 3J), suggesting that sumoylation of Prdm16 by Cbx4 is a prerequisite for Ehmt1-mediated stabilization. These results reveal that Cbx4 and Ehmt1 act synergistically to stabilize Prdm16 in a sumoylation activity-dependent manner.

Induction of Ucp1 Expression by Cbx4 Is Both Sumoylation Activity Dependent and Prdm16 Dependent

We investigated the biological relevance of sumoylation of Prdm16 by Cbx4 in adipocyte culture. First, we performed immunoprecipitation experiments in brown adipocytes stably expressing FLAG-tagged Cbx4, and we found that endogenous Prdm16 was present in FLAG-Cbx4 immunoprecipitates (Figure 4A). Next, we examined whether endogenous Prdm16 is sumoylated in brown adipocytes. To facilitate the detection, HA-SUMO2 was stably expressed. As shown in Figure 4B, adenoviral expression of Cbx4, but not the ΔSIM1 mutant, promoted sumoylation of endogenous Prdm16. These data are in support of our observation that knockdown of Cbx4 in brown adipocytes decreased Prdm16 protein level and thermogenic gene expression (Figures 2A and 2B).

To further establish the functional role of Cbx4-mediated sumoylation, we overexpressed Cbx4 in differentiated primary iWAT adipocytes. Adenoviral expression of wild-type Cbx4 increased endogenous Prdm16 protein level and promoted Ucp1 and Cidea expression, whereas the ΔSIM1 mutant had no effect (Figures 4C and 4D), demonstrating a requirement of Cbx4 sumoylation activity. As a complementary approach, we then overexpressed Prdm16 K917R mutant through lentiviral infection in preadipocytes, and cells were differentiated. We found that induction of Ucp1 and Cidea was significantly impaired in adipocytes expressing K917R mutant compared with adipocytes expressing wild-type Prdm16 (Figure 4E). Importantly, K917R mutant had a similar mRNA level as wild-type Prdm16 but a much lower protein level (Figures 4E and 4F), indicating that K917 mutant protein is highly liable to be degraded. Finally, to determine whether induction of Ucp1 and Cidea by Cbx4 is mediated through Prdm16, we expressed Cbx4 in Prdm16-knockdown brown adipocytes. Knockdown of Prdm16 abolished Cbx4-induced Ucp1 and Cidea expression (Figures 4G and 4H). These results suggest that Cbx4 promotes Ucp1 and Cidea expression through sumoylating Prdm16, primarily at Lys 917.

Cbx4 Is Required for Thermogenic Gene Expression in Neonatal BAT

As noted previously (Liu et al., 2013), Cbx4-null mice died almost immediately after birth. We observed no difference of thermogenic gene expression in classical BAT between adult heterozygous mice and control mice. To determine whether Cbx4 is important at an early stage of BAT development, we collected BAT from neonatal mice within 5 hr after they were born. BAT from Cbx4-null neonatal mice had a similar morphology, assayed by H&E staining (Figure S4A), and similar expression levels of common fat genes, such as aP2 and adiponectin (Figure 5A), compared with BAT from control littermates. However, levels of BAT-selective gene Ucp1 and Cidea were significantly lower in the null mice (Figure 5A). Western blot analysis showed a reduction of Prdm16 and Ucp1 protein levels (Figure 5B). Interestingly, WAT gene marker leptin was upregulated (Figure 5A). Immunofluorescence staining confirmed the loss of Ucp1 expression in the BAT of the null mice (Figure 5C). These results were recapitulated in BAT isolated from 18.5-day embryos (Figure S4B). We next examined whether these observed effects were cell autonomous. Given the difficulty to obtain a reasonable number of live Cbx4-null neonatal mice for cell culture, we generated primary brown preadipocytes from Cbx4-heterozygous neonatal mice and differentiated them *in vitro*. These cells displayed lower Ucp1 and Cidea expression (Figure 5D), similar to what we observed in Cbx4-knockdown adipocytes (Figure 2A). These data showed that Cbx4 is cell-autonomously required for Ucp1 and Cidea expression in BAT, at least at embryonic and neonatal stages.

Cbx4-Heterozygous Mice Display a Similar Metabolic Phenotype as Prdm16-Knockout Mice

Given that Prdm16-knockout mice have impaired iWAT browning and display metabolic dysfunction (Cohen et al., 2014), we examined phenotypes of Cbx4-heterozygous mice. In agreement with our finding that Cbx4 stabilizes Prdm16 protein, we observed that Prdm16 protein level, but not its mRNA level, was decreased in BAT and iWAT (Figure 6A). On a chow diet, at young age, no phenotypic difference was observed between heterozygous and control mice. However, aged heterozygous mice developed cold intolerance (Figure 6B) and glucose intolerance (Figure 6C), associated with decreased Ucp1 expression (Figures 6D and 6E) and *ex vivo* oxygen consumption in iWAT (Figure 6F). No difference of insulin tolerance was observed in aged heterozygous mice (Figure S5A). We next challenged 7-week-old mice with a high-fat diet. We found that iWAT mass was significantly increased in heterozygous mice, while total body weight, visceral fat mass, and BAT mass were unchanged (Figure 6G; Figure S5B). These mice had deteriorated glucose tolerance (Figure 6H) but normal insulin tolerance (Figure S5C). Moreover, the expanded iWAT expressed a higher level of inflammation genes that are typically enriched in visceral fat (Figure 6I). Interestingly, the selective expansion of iWAT depot, its increased expression of inflammation genes, and

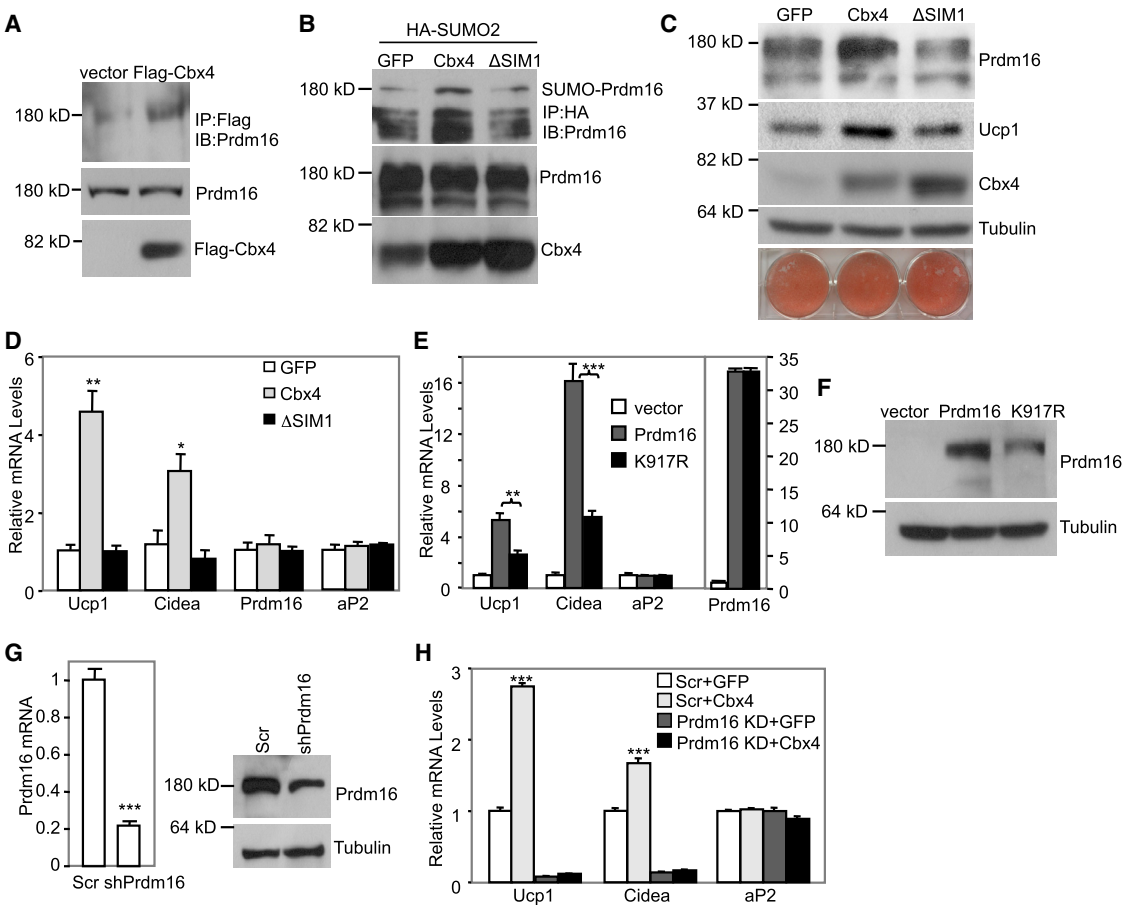

Figure 4. Cbx4 Promotes Ucp1 and Cidea Expression through Sumoylating Prdm16

(A) Brown preadipocytes were infected with FLAG-Cbx4 lentivirus and differentiated. Endogenous Prdm16 protein was examined in the FLAG-Cbx4 immmunoprecipitates.

(B) Brown preadipocytes were infected with HA-SUMO2 lentivirus; differentiated; and then infected with GFP, Cbx4, or ΔSIM1 adenovirus. Sumoylation of endogenous Prdm16 was assayed.

(C) Differentiated primary iWAT adipocytes were infected with GFP, Cbx4, or ΔSIM1 adenovirus. The oil red O staining of triglycerides and western blot of Prdm16 and Ucp1 protein were performed.

(D) Gene expression analysis of WAT adipocytes generated as in (C) (n = 3). Data represent mean ± SEM. *p < 0.05 and **p < 0.01.

(E and F) Gene expression (E, n = 4) and western blot (F) analyses in WAT adipocytes overexpressing wild-type or K917R mutant Prdm16. Data represent mean ± SEM. **p < 0.01 and ***p < 0.001.

(G) Prdm16 mRNA (n = 3) and protein were analyzed in brown adipocytes infected with Prdm16 shRNA lentivirus. Data represent mean ± SEM. ***p < 0.001.

(H) Brown adipocytes were infected with Prdm16 shRNA lentivirus, differentiated, and then infected with GFP or Cbx4 expression adenovirus. Gene expression was analyzed (n = 4). Data represent mean ± SEM. ***p < 0.001, Scr + Cbx4 versus Scr + GFP.

glucose intolerance was also observed in Prdm16-knockout mice on a high-fat diet (Cohen et al., 2014). These results indicate that a reduction of Prdm16 protein caused by Cbx4 haploinsufficiency results in impaired thermogenic gene expression in iWAT, which potentially contributes to iWAT expansion and deteriorated glucose and cold tolerance.

Fat-Specific Cbx4 Knockdown and Overexpression through Viral Injection Regulate Prdm16 Protein Level and Remodel iWAT

To further confirm that the decreased Prdm16 and Ucp1 levels in iWAT of Cbx4-heterozygous mice are fat-autonomous effects, we injected Cbx4-knockdown or scramble control adenovirus into the left and right iWAT pads of wild-type mice, respectively, as described (Huang et al., 2017; Kusminski et al., 2014). One week after the initial injection, fat tissues were collected. Strikingly, Prdm16 protein level, but not its mRNA level, was strongly decreased in iWAT pads with Cbx4 knockdown (Figures 7A and 7B). This was associated with a remarkable reduction of Ucp1 and Cidea expression (Figure 7B). The adipocytes were larger and were mostly Ucp1 negative, resembling a typical visceral-like WAT (Figures 7C and 7D). We then performed gain-of-function studies by injection of Cbx4-overexpression adenovirus. Overexpression of Cbx4 in iWAT pads elevated Prdm16 protein level (Figure 7E) and produced a brown-like phenotype, including increased Ucp1 and Cidea expression and smaller

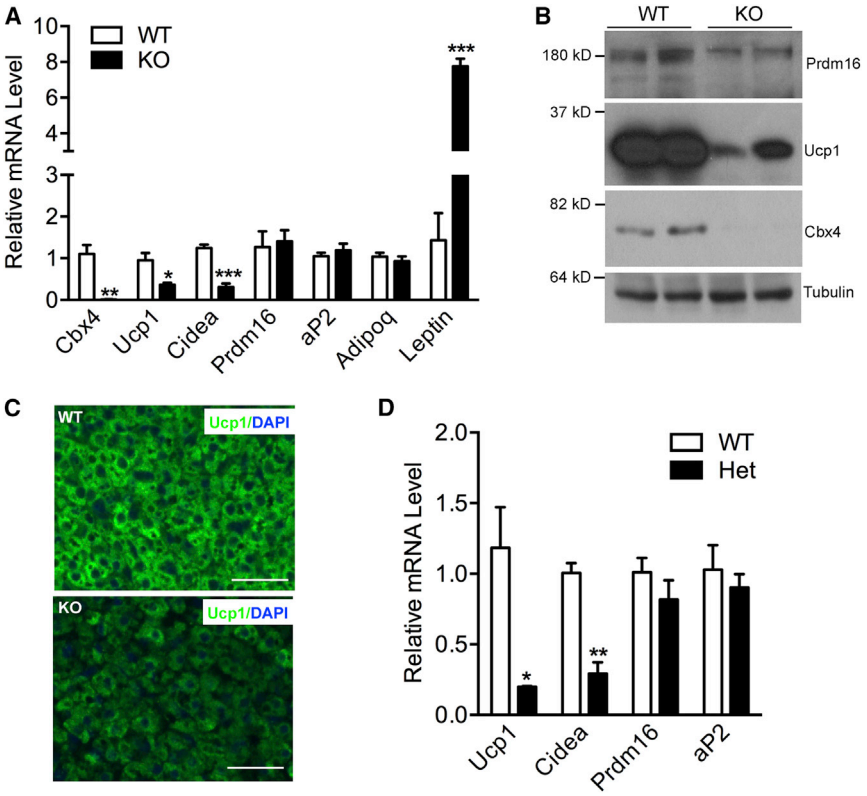

Figure 5. Cbx4 Is Required for Ucp1 Expression in Neonatal BAT

(A) qPCR analysis of gene expression in the BAT of neonatal Cbx4-null mice (n = 4 mice) and littermate controls (n = 5 mice). Data represent mean ± SEM. *p < 0.05, **p < 0.01, and ***p < 0.001.

(B) Prdm16 and Ucp1 protein examined in the BAT of neonatal Cbx4-null mice.

(C) Ucp1 immunofluorescence staining of the BAT of neonatal mice. Shown are representative images of three mice per genotype. Scale bar, 200 μm.

(D) qPCR analysis of gene expression in primary BAT adipocytes isolated from heterozygous Cbx4-knockout mice and littermate controls (n = 3 mice/group). Data represent mean ± SEM. *p < 0.05 and **p < 0.01.

adipocytes that were almost all Ucp1 positive (Figures 7F–7H). Thus, Cbx4 knockdown and overexpression through viral delivery directly led to opposite remodeling of iWAT *in vivo*, supporting the fat-autonomous effects of Cbx4. Importantly, the browning phenotype elicited by wild-type Cbx4 expression was not observed when expressing the ΔSIM1 mutant (Figures 7E–7H), providing strong *in vivo* evidence that Cbx4 sumoylation activity controls Prdm16 protein level and iWAT browning.

DISCUSSION

Thermogenic gene expression in BAT and beige adipocytes is controlled by transcriptional regulators. However, post-transcriptional mechanisms that modulate the activity and function of these regulators were poorly understood. Our work identifies Cbx4 as a SUMO E3 ligase for Prdm16. Sumoylation of Prdm16 by Cbx4, primarily at Lys 917, blocks ubiquitination-mediated degradation and, hence, markedly augments its stability. Functionally, we show that Cbx4 sumoylation activity, at least in part through Prdm16, regulates thermogenic gene expression and iWAT browning.

We have previously shown that H3K27me3 modification deposited by PRC2 marks a significant subset of BAT-selective genes, including Prdm16 in preadipocytes (Pan et al., 2015). Interestingly, as a PRC1 subunit, Cbx4 is modified by H3K27me3 in preadipoytes as well. During brown adipocyte differentiation, H3K27me3 is erased to activate Cbx4 and Prdm16 gene expression; this coordinated expression allows Prdm16 protein to be stabilized by Cbx4. Thus, while PRC2 represses the BAT gene program, Cbx4, in a PRC1-independent manner, has the opposite effect through sumoylating Prdm16. It is currently unknown what roles, if any, PRC1 plays in BAT and beige adipocyte development.

Ectopic expression of Ehmt1 (Ohno et al., 2013) or treatment of adipocytes with PPARγ full agonists (Ohno et al., 2012) stabilizes Prdm16 through the inhibition of ubiquitination; however, how this is accomplished has been obscure. Our work reveals an interesting interplay between sumoylation and ubiquitination of Prdm16, and it helps us to further understand how Prdm16 stability is controlled. Sumoylation and ubiquitination might compete for a common set of lysine residues. Alternatively, sumoylation may affect ubiquitination at other lysine residues. Although we cannot completely rule out the first possibility, our data are in support of the latter scenario, as Cbx4-mediated blockage of Prdm16 ubiquitination is relieved when the SUMO acceptor site K917 is mutated. This scenario is also relevant in the context of Ehmt1. We found that the ability of Ehmt1 to stabilize Prdm16 depends on the presence of Cbx4 and its sumoylation activity. Cbx4 does not sumoylate Ehmt1, and Ehmt1 does not enhance Cbx4 sumoylation activity for Prdm16. Instead, our data indicate that, while sumoylation of Prdm16 by Cbx4 certainly increases Prdm16 stability in its own right, this sumoylation might additionally serve as a priming event that allows Ehmt1 to further block ubiquitination of Prdm16 at other lysine residues. In the case of PPARγ agonists, we found that treatment of iWAT adipocytes with rosiglitazone induces the expression of Cbx4 (Figure S6A) and stabilizes Prdm16 at a level similar to as observed in Cbx4 expression (Figure S6B), consistent with the idea that stabilization of Prdm16 protein by PPARγ agonists is mediated through gene induction that inhibits its ubiquitination (Ohno et al., 2012). These results together indicate an integral role of Cbx4 in the control of Prdm16 stability.

Our studies reveal an *in vivo* requirement of Cbx4 for thermogenic gene expression. Consistent with our *in vitro* findings, we

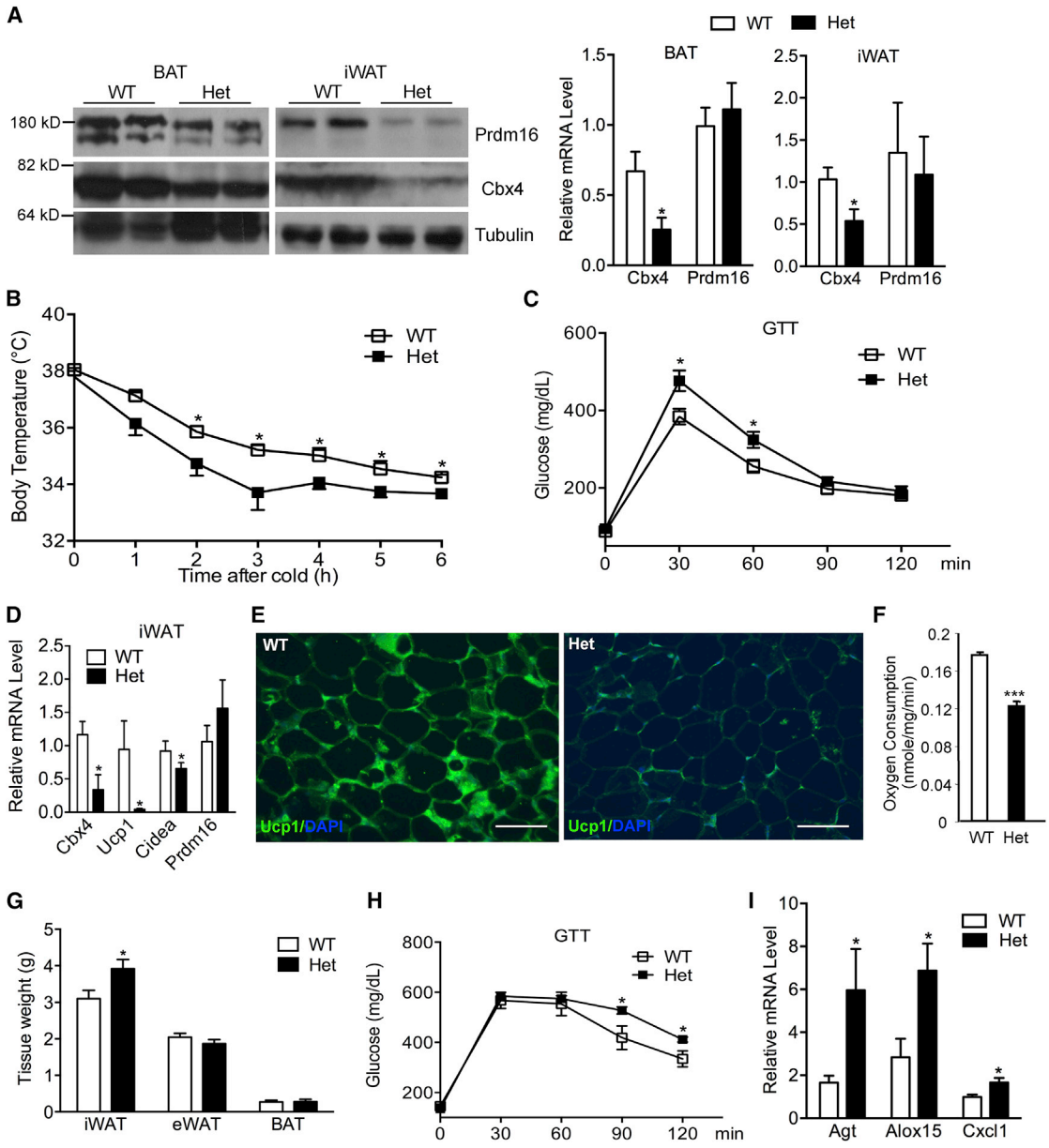

Figure 6. Cbx4 Haploinsufficiency Causes a Reduction of Prdm16 Protein and Impaired iWAT Browning, Leading to iWAT Expansion and Deteriorated Glucose and Cold Tolerance

(A) Analysis of Prdm16 and Cbx4 protein and mRNA (n = 4 mice/group) from 8-week-old male Cbx4-heterozygous mice and control littermates. Data represent mean ± SEM. *p < 0.05.

(B) Body temperature of 10-month-old male Cbx4-heterozygous mice (n = 8 mice) and control littermates (n = 7 mice) at 4°C. Data represent mean ± SEM. *p < 0.05.

(C) Glucose tolerance test in a second cohort of 10-month-old male Cbx4-heterozygous mice (n = 6 mice) and control littermates (n = 8 mice). Data represent mean ± SEM. *p < 0.05.

(D) Gene expression in iWAT of 10-month-old male Cbx4-heterozygous mice and control littermates (n = 4 mice/group). Data represent mean ± SEM. *p < 0.05.

(E) Ucp1 immunofluorescence staining of iWAT of 10-month-old male mice. Shown are representative images of three mice per genotype. Scale bar, 200 μm.

(F) Oxygen consumption of iWAT isolated from 8-month-old male Cbx4-heterozygous mice and control littermates (n = 5 mice/group). Data represent mean ± SEM. ***p < 0.001.

(G) Fat mass of male Cbx4-heterozygous mice (n = 7 mice) and control littermates (n = 5 mice) on a high-fat diet for 25 weeks. Data represent mean ± SEM. *p < 0.05.

(H) Glucose tolerance test of mice in (G) after 24-week high-fat diet. Data represent mean ± SEM. *p < 0.05.

(I) Inflammation gene expression in iWAT of mice in (G). *p < 0.05.

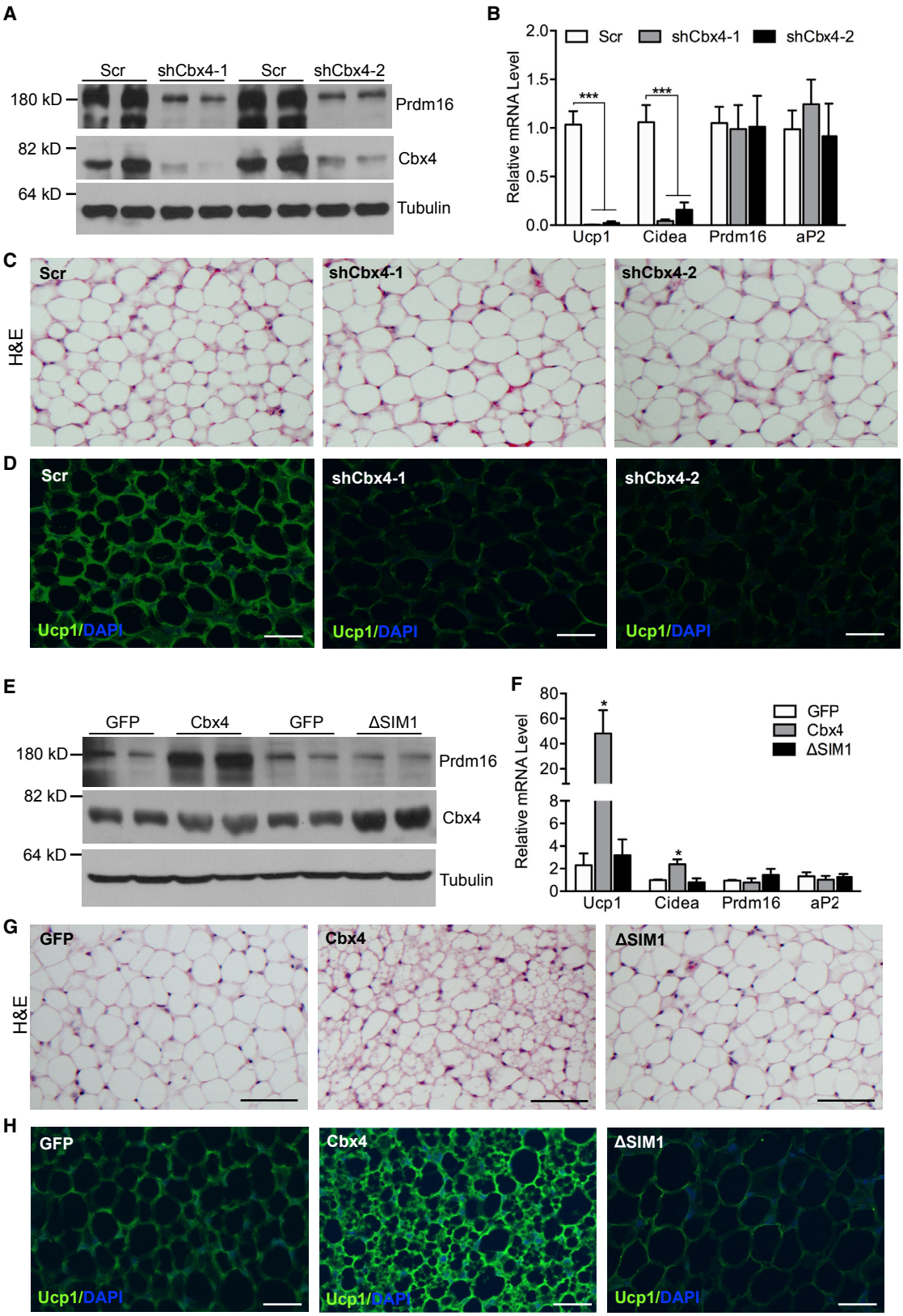

(legend on next page)

found that Cbx4-heterozygous knockout mice display a decreased Prdm16 protein level, but not its mRNA level, in both classical BAT and iWAT. While Cbx4 is essential for thermogenic gene expression in BAT at embryonic and neonatal stages, adult Cbx4-heterozygous mice are defective in iWAT browning. The heterozygous animals are cold sensitive and glucose intolerant, and they display a high-fat diet-induced iWAT expansion accompanied with elevated expression of inflammation genes. These phenotypes are reminiscent of those of fat-specific Prdm16-knockout mice (Cohen et al., 2014), further indicating a mechanistic connection between Cbx4 and Prdm16. Indeed, our *in vitro* cell culture studies and *in vivo* fat-specific virus injection studies support the idea that the defect of iWAT browning in Cbx4-heterozygous mice is fat autonomous, attributed to haploinsufficiency in iWAT and not in other tissues. In particular, we show that acute knockdown or overexpression of Cbx4 in iWAT pads through viral injection has a strong impact on Prdm16 protein level and leads to a robust remodeling of iWAT, which critically depend on Cbx4 sumoylation activity. Collectively, our work identifies Cbx4-mediated Prdm16 sumoylation as a major regulatory mechanism underlying iWAT browning and thermogenesis, and it raises the idea that small molecules that enhance Cbx4 sumoylation activity toward Prdm16 may have therapeutic potential for metabolic diseases.

EXPERIMENTAL PROCEDURES

Animals

All animal experiments were performed according to procedures approved by the UMASS Medical School's Institutional Animal Care and Use Committee (IACUC). Heterozygous Cbx4-deficient mice were obtained from KOMP. Normal diet containing 4% (w/w) fat and high-fat diet containing 35% (w/w) fat (S3282) were purchased from Harlan Teklad and Bioserv, respectively. β3-adrenergic agonist CL316,243 (Tocris, 1499) was intraperitoneally injected into mice at 1 mg/kg body weight. For glucose tolerance test, glucose was intraperitoneally injected into mice at 2 g/kg body weight after 15-hr fasting. For insulin tolerance test, insulin was intraperitoneally injected into mice at 0.75 U/kg body weight after 5-hr fasting. For acute cold exposure, mice were individually caged with food withdrawn and water provided, placed in a 4°C cold room, and core body temperature was measured with the Microtherma 2 rectal probe (Thermoworks). Sex-matched littermates were used as controls in all experiments with age indicated.

Adipocyte Culture, Differentiation, and Treatment

Immortalized BAT preadipocytes were generated previously (Pan et al., 2009). Primary BAT preadipocytes were isolated from neonatal mice. Primary iWAT preadipocytes were isolated from 2-week-old mice. Tissues were digested with collagenase and differentiated into mature adipocytes as described previously (Huang et al., 2017; Pan et al., 2015). Cells that displayed at least 95% differentiation efficiency were used in experiments.

Plasmids and Viruses

Full-length mouse Cbx4 cDNA and mutants were generated by PCR. Full-length mouse Prdm16 cDNA and mouse Ehmt1 cDNA were obtained from Addgene and Dharmacon, respectively. Prdm16 mutants (Lys to Arg) were generated by PCR. All plasmids were verified by sequencing. Adenoviral Cbx4 knockdown (mouse) (small hairpin RNA [shRNA]1, 5′CGGCAAGTATTATTATCAGCT3′; shRNA2, 5′CGTGATCGTTATGAGCAAGTA3′) and overexpression plasmid were constructed using AdEasy-1 system (He et al., 1998). Adenoviruses were purified with cesium chloride ultracentrifugation. Prdm16 shRNA-knockdown (mouse) (5′GAAGAGCGTGAGTACAAAT3′) and Cbx4 shRNA-knockdown (monkey) lentiviral constructs (shRNA1, 5′CAAGAACAAGAACGGACGCAT3′; shRNA2, 5′TCCAGGCAAAGGCTCCGAGAA3′) were generated using psp-108 vector (Addgene), and lentiviruses were produced by co-transfection along with plasmids pMD2.G (Addgene) and psPAX2 (Addgene) into HEK293T cells. Lentiviral constructs expressing Prdm16 and K917R mutant, FLAG-Cbx4, and HA-SUMO2 were generated via recombination of pENTR1A into pLenti CMV/TO Puro DEST (Addgene), and lentiviruses were produced by co-transfection along with plasmids pLP1, pLP2, and pVSVG into HEK293 cells. All viral titers were predetermined, and the same number of viral particles was used for experimental and control samples. Differentiating adipocytes were infected with adenoviruses at 100% infection efficiency. Preadipocytes were infected with lentiviruses, selected with puromycin, and re-plated for differentiation.

Gene Expression Analysis

Total RNA was isolated from cells or tissues using TRIzol reagent (Invitrogen, 15596-018), according to the manufacturer's instructions. Reverse transcription reactions were performed using an IScript cDNA synthesis kit (Invitrogen). The sequences of primers used in this study are available upon request. Real-time qPCR was performed with SYBR green fluorescent Dye (Bio-Rad) using an ABI7300 PCR machine, and U36 was used as an internal control. Relative mRNA expression was determined by the ΔΔ-Ct method.

Prdm16 Stability and Interaction with Cbx4 in Transfected Cells

To determine Prdm16 half-life time, HEK293 cells expressing FLAG-Prdm16 and Cbx4 or vector control were incubated with a medium containing 60 μg/mL cycloheximide (Sigma, C7698) for up to 32 hr. Total cell lysates were isolated and separated by SDS-PAGE. Antibodies against FLAG (Sigma, F7425) and β-tubulin Tubulin (DSHB, E7-S) were used for western blotting.

To determine interaction, HEK293 cells were co-transfected with HA- or FLAG-tagged Prdm16 and Cbx4 or vector control. Amounts of Prdm16 plasmids used for transfection were adjusted to bring the input of Prdm16 protein to a similar level in all treatments. Cell lysates were immunoprecipitated with anti-HA Antibody beads (HC-7) (Santa Cruz Biotechnology, sc-7392 AC) or Anti-FLAG M2 Affinity Gel (Sigma, A2220). Immunoprecipitates were separated by SDS-PAGE, and Cbx4 antibody (Millipore, 09-084) was used for western blotting.

Western Blot Analysis in Adipocytes

To detect endogenous Prdm16 and Cbx4 protein, cultured adipocytes or adipose tissue samples with equal amounts were homogenized in lysis buffer (100 mM NaCl, 50 mM Tris [pH 7.5], 0.5% Triton X-100, and 5% [w/v] glycerol). Lysates were cleared at 12,000 × *g* for 10 min. Supernatants were quantified

Figure 7. Fat-Specific Cbx4 Knockdown and Overexpression through Viral Injection Regulate Prdm16 Protein Level and Remodel iWAT

(A) Prdm16 and Cbx4 protein levels in iWAT after the injection of Cbx4-knockdown adenoviruses.

(B) Gene expression in iWAT injected with Cbx4-knockdown adenoviruses (n = 4 mice/group). Data represent mean ± SEM. ***p < 0.001, one-way ANOVA.

(C) H&E staining of iWAT injected with Cbx4-knockdown adenoviruses. Shown are representative images of three mice per group. Scale bar, 200 μm.

(D) Ucp1 immunofluorescence staining of iWAT injected with Cbx4-knockdown adenoviruses. Shown are representative images of three mice per group. Scale bar, 200 μm.

(E) Prdm16 and Cbx4 protein levels in iWAT after the injection of wild-type or mutant Cbx4 adenoviruses.

(F) Gene expression in iWAT injected with wild-type or mutant Cbx4 adenoviruses (n = 4 mice/group). Data represent mean ± SEM. *p < 0.05, Cbx4 versus GFP.

(G) H&E staining of iWAT injected with wild-type or mutant Cbx4 adenoviruses. Shown are representative images of three mice per group. Scale bar, 200 μm.

(H) Ucp1 immunofluorescence staining of iWAT injected with wild-type or mutant Cbx4 adenoviruses. Shown are representative images of three mice per group. Scale bar, 200 μm.

for protein content, separated by SDS-PAGE, and immunoblotted with antibodies against Prdm16 (R&D Systems, AF6295), Cbx4 (Millipore, 09-084), or Tubulin (DSHB, E7-S).

To detect Cbx4 and Prdm16 interaction in brown adipocytes, preadipocytes were infected with FLAG-Cbx4 lentivirus at a 10% infection efficiency to ensure single-copy integration, and the cells were differentiated into adipocytes. Immunoprecipitation was performed with anti-FLAG beads (Sigma, A2220), and the presence of Prdm16 in the immunoprecipitates was examined by western blot with an anti-Prdm16 antibody (R&D Systems, AF6295).

Sumoylation and Ubiquitination Assays and Western Blot Analysis

For the sumoylation assay, HEK293 cells expressing HA-tagged SUMO2 (Addgene, 48967), UBC9 (Addgene, 20082), FLAG-tagged Prdm16, Cbx4, or vector were treated with 10 μM MG132 (Sigma, M7449) for 16 hr. After being immunoprecipitated with anti-HA Antibody beads (HC-7) (Santa Cruz Biotechnology, sc-7392 AC), proteins were separated by SDS-PAGE, and an FLAG antibody (Sigma, F7425) was used for western blotting. For the ubiquitination assay, HEK293 cells expressing FLAG-tagged Ubiquitin, HA-tagged Prdm16, Cbx4, or vector were treated with 10 μM MG132 for 16 hr. After being immunoprecipitated with anti-FLAG M2 Affinity Gel (Sigma, A2220), proteins were separated by SDS-PAGE, and an HA antibody (Sigma, 12013819001) was used for western blotting.

For the sumoylation assay in brown adipocytes, preadipocytes were infected with HA-SUMO2 lentivirus and differentiated. The differentiated adipocytes were then infected with Cbx4 adenovirus and treated with 10 μM MG132 for 12 hr. After being immunoprecipitated with anti-HA beads, proteins were separated by SDS-PAGE, and anti-Prdm16 antibody (R&D Systems, AF6295) was used for western blotting.

In Vivo Adenovirus Injection into iWAT

3-month-old male wild-type C56BL6 mice were used. Each iWAT pad was injected with adenoviruses at 5 different sites with 1×10^{10} transducing units per site to cover the whole pad. Experimental viruses and control viruses were injected into the left fat pad and right fat pad of the same animal, respectively, as described (Huang et al., 2017; Kusminski et al., 2014). One week after injection, the mice were sacrificed and the iWAT tissues were obtained.

Histology and Immunofluorescence

Tissues were fixed with 10% formalin and were paraffin-embedded. H&E staining was performed according to standard procedures. For immunofluorescence staining, formalin-fixed and paraffin-embedded tissue sections were deparaffinized and rehydrated through graded ethanol solutions. After pre-incubation with a blocking buffer (PBS containing 5% normal goat serum and 0.3% Triton X-100) for 60 min, slides were incubated with Ucp1 antibody (Sigma, U6382) (1:500 dilution) in blocking buffer at 4°C overnight. Subsequently, the slides were washed and incubated with Alexa Flour 488-conjugated secondary antibody and DAPI for 60 min. Images were acquired and processed with the same setting for knockout mice and control littermates.

Statistical Analysis

Unless otherwise stated, data were expressed as mean ± SEM and analyzed using a two-tailed Student's t test; n represents biological samples. Statistical significance was shown as $^{*}p < 0.05$, $^{**}p < 0.01$, or $^{***}p < 0.001$.

SUPPLEMENTAL INFORMATION

Supplemental Information includes six figures and can be found with this article online at https://doi.org/10.1016/j.celrep.2018.02.057.

ACKNOWLEDGMENTS

We thank the Morphological Core at University of Massachusetts Medical School for technical help. This work was supported by NIH/NIDDK (R01DK076118 and R01DK098594).

AUTHOR CONTRIBUTIONS

Q.C., L.H., and D.P. designed and performed the experiments and analyzed the data. L.J.Z. performed bioinformatics analysis. Y.-X.W. designed the experiments and analyzed the data. Q.C. and Y.-X.W. wrote the manuscript.

DECLARATION OF INTERESTS

The authors declare no competing interests.

Received: May 22, 2017
Revised: January 2, 2018
Accepted: February 13, 2018
Published: March 13, 2018

REFERENCES

Boyer, L.A., Plath, K., Zeitlinger, J., Brambrink, T., Medeiros, L.A., Lee, T.I., Levine, S.S., Wernig, M., Tajonar, A., Ray, M.K., et al. (2006). Polycomb complexes repress developmental regulators in murine embryonic stem cells. Nature *441*, 349–353.

Bracken, A.P., and Helin, K. (2009). Polycomb group proteins: navigators of lineage pathways led astray in cancer. Nat. Rev. Cancer *9*, 773–784.

Cannon, B., and Nedergaard, J. (2004). Brown adipose tissue: function and physiological significance. Physiol. Rev. *84*, 277–359.

Chen, K.Y., Cypess, A.M., Laughlin, M.R., Haft, C.R., Hu, H.H., Bredella, M.A., Enerbäck, S., Kinahan, P.E., Lichtenbelt, Wv., Lin, F.I., et al. (2016). Brown Adipose Reporting Criteria in Imaging STudies (BARCIST 1.0): Recommendations for Standardized FDG-PET/CT Experiments in Humans. Cell Metab. *24*, 210–222.

Cohen, P., Levy, J.D., Zhang, Y., Frontini, A., Kolodin, D.P., Svensson, K.J., Lo, J.C., Zeng, X., Ye, L., Khandekar, M.J., et al. (2014). Ablation of PRDM16 and beige adipose causes metabolic dysfunction and a subcutaneous to visceral fat switch. Cell *156*, 304–316.

Creppe, C., Palau, A., Malinverni, R., Valero, V., and Buschbeck, M. (2014). A Cbx8-containing polycomb complex facilitates the transition to gene activation during ES cell differentiation. PLoS Genet. *10*, e1004851.

Frangini, A., Sjöberg, M., Roman-Trufero, M., Dharmalingam, G., Haberle, V., Bartke, T., Lenhard, B., Malumbres, M., Vidal, M., and Dillon, N. (2013). The aurora B kinase and the polycomb protein ring1B combine to regulate active promoters in quiescent lymphocytes. Mol. Cell *51*, 647–661.

Gareau, J.R., and Lima, C.D. (2010). The SUMO pathway: emerging mechanisms that shape specificity, conjugation and recognition. Nat. Rev. Mol. Cell Biol. *11*, 861–871.

Giordano, A., Smorlesi, A., Frontini, A., Barbatelli, G., and Cinti, S. (2014). White, brown and pink adipocytes: the extraordinary plasticity of the adipose organ. Eur. J. Endocrinol. *170*, R159–R171.

Harms, M., and Seale, P. (2013). Brown and beige fat: development, function and therapeutic potential. Nat. Med. *19*, 1252–1263.

Harms, M.J., Ishibashi, J., Wang, W., Lim, H.W., Goyama, S., Sato, T., Kurokawa, M., Won, K.J., and Seale, P. (2014). Prdm16 is required for the maintenance of brown adipocyte identity and function in adult mice. Cell Metab. *19*, 593–604.

He, T.C., Zhou, S., da Costa, L.T., Yu, J., Kinzler, K.W., and Vogelstein, B. (1998). A simplified system for generating recombinant adenoviruses. Proc. Natl. Acad. Sci. USA *95*, 2509–2514.

Huang, L., Pan, D., Chen, Q., Zhu, L.J., Ou, J., Wabitsch, M., and Wang, Y.X. (2017). Transcription factor Hlx controls a systematic switch from white to brown fat through Prdm16-mediated co-activation. Nat. Commun. *8*, 68.

Johnson, E.S. (2004). Protein modification by SUMO. Annu. Rev. Biochem. *73*, 355–382.

Kagey, M.H., Melhuish, T.A., and Wotton, D. (2003). The polycomb protein Pc2 is a SUMO E3. Cell *113*, 127–137.

Kajimura, S., Spiegelman, B.M., and Seale, P. (2015). Brown and Beige Fat: Physiological Roles beyond Heat Generation. Cell Metab. *22*, 546–559.

Ku, M., Koche, R.P., Rheinbay, E., Mendenhall, E.M., Endoh, M., Mikkelsen, T.S., Presser, A., Nusbaum, C., Xie, X., Chi, A.S., et al. (2008). Genomewide analysis of PRC1 and PRC2 occupancy identifies two classes of bivalent domains. PLoS Genet. *4*, e1000242.

Kusminski, C.M., Park, J., and Scherer, P.E. (2014). MitoNEET-mediated effects on browning of white adipose tissue. Nat. Commun. *5*, 3962.

Lamoliatte, F., Caron, D., Durette, C., Mahrouche, L., Maroui, M.A., Caron-Lizotte, O., Bonneil, E., Chelbi-Alix, M.K., and Thibault, P. (2014). Large-scale analysis of lysine SUMOylation by SUMO remnant immunoaffinity profiling. Nat. Commun. *5*, 5409.

Leeb, M., Pasini, D., Novatchkova, M., Jaritz, M., Helin, K., and Wutz, A. (2010). Polycomb complexes act redundantly to repress genomic repeats and genes. Genes Dev. *24*, 265–276.

Li, J., Xu, Y., Long, X.D., Wang, W., Jiao, H.K., Mei, Z., Yin, Q.Q., Ma, L.N., Zhou, A.W., Wang, L.S., et al. (2014). Cbx4 governs HIF-1α to potentiate angiogenesis of hepatocellular carcinoma by its SUMO E3 ligase activity. Cancer Cell *25*, 118–131.

Liu, B., Liu, Y.F., Du, Y.R., Mardaryev, A.N., Yang, W., Chen, H., Xu, Z.M., Xu, C.Q., Zhang, X.R., Botchkarev, V.A., et al. (2013). Cbx4 regulates the proliferation of thymic epithelial cells and thymus function. Development *140*, 780–788.

Luis, N.M., Morey, L., Mejetta, S., Pascual, G., Janich, P., Kuebler, B., Cozutto, L., Roma, G., Nascimento, E., Frye, M., et al. (2011). Regulation of human epidermal stem cell proliferation and senescence requires polycomb- dependent and -independent functions of Cbx4. Cell Stem Cell *9*, 233–246.

Nishikata, I., Nakahata, S., Saito, Y., Kaneda, K., Ichihara, E., Yamakawa, N., and Morishita, K. (2011). Sumoylation of MEL1S at lysine 568 and its interaction with CtBP facilitates its repressor activity and the blockade of G-CSF-induced myeloid differentiation. Oncogene *30*, 4194–4207.

Ohno, H., Shinoda, K., Spiegelman, B.M., and Kajimura, S. (2012). PPARγ agonists induce a white-to-brown fat conversion through stabilization of PRDM16 protein. Cell Metab. *15*, 395–404.

Ohno, H., Shinoda, K., Ohyama, K., Sharp, L.Z., and Kajimura, S. (2013). EHMT1 controls brown adipose cell fate and thermogenesis through the PRDM16 complex. Nature *504*, 163–167.

Pan, D., Fujimoto, M., Lopes, A., and Wang, Y.X. (2009). Twist-1 is a PPARdelta-inducible, negative-feedback regulator of PGC-1alpha in brown fat metabolism. Cell *137*, 73–86.

Pan, D., Huang, L., Zhu, L.J., Zou, T., Ou, J., Zhou, W., and Wang, Y.X. (2015). Jmjd3-Mediated H3K27me3 Dynamics Orchestrate Brown Fat Development and Regulate White Fat Plasticity. Dev. Cell *35*, 568–583.

Rodriguez, M.S., Dargemont, C., and Hay, R.T. (2001). SUMO-1 conjugation in vivo requires both a consensus modification motif and nuclear targeting. J. Biol. Chem. *276*, 12654–12659.

Rosen, E.D., and Spiegelman, B.M. (2014). What we talk about when we talk about fat. Cell *156*, 20–44.

Seale, P., Kajimura, S., Yang, W., Chin, S., Rohas, L.M., Uldry, M., Tavernier, G., Langin, D., and Spiegelman, B.M. (2007). Transcriptional control of brown fat determination by PRDM16. Cell Metab. *6*, 38–54.

Seale, P., Conroe, H.M., Estall, J., Kajimura, S., Frontini, A., Ishibashi, J., Cohen, P., Cinti, S., and Spiegelman, B.M. (2011). Prdm16 determines the thermogenic program of subcutaneous white adipose tissue in mice. J. Clin. Invest. *121*, 96–105.

Simon, J.A., and Kingston, R.E. (2009). Mechanisms of polycomb gene silencing: knowns and unknowns. Nat. Rev. Mol. Cell Biol. *10*, 697–708.

Sparmann, A., and van Lohuizen, M. (2006). Polycomb silencers control cell fate, development and cancer. Nat. Rev. Cancer *6*, 846–856.

Surface, L.E., Thornton, S.R., and Boyer, L.A. (2010). Polycomb group proteins set the stage for early lineage commitment. Cell Stem Cell *7*, 288–298.

Tan, J., Jones, M., Koseki, H., Nakayama, M., Muntean, A.G., Maillard, I., and Hess, J.L. (2011). CBX8, a polycomb group protein, is essential for MLL-AF9-induced leukemogenesis. Cancer Cell *20*, 563–575.

Cell Reports, Volume *22*

Supplemental Information

Cbx4 Sumoylates Prdm16 to Regulate Adipose Tissue Thermogenesis

Qingbo Chen, Lei Huang, Dongning Pan, Lihua J. Zhu, and Yong-Xu Wang

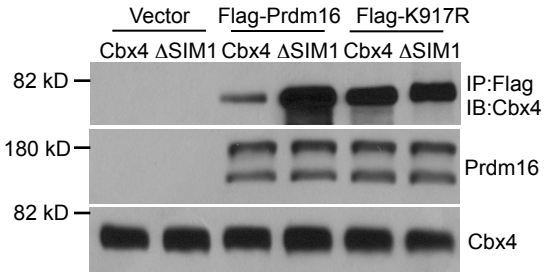

Figure S1, related to Figure 3. Prdm16 K917R mutant interacts with Cbx4. HEK293 cells were co-transfected with indicated plasmids. Immunoprecipitation was performed with anti-Flag beads, and presence of Cbx4 in the immunoprecipitate complex was examined with an anti-Cbx4 antibody.

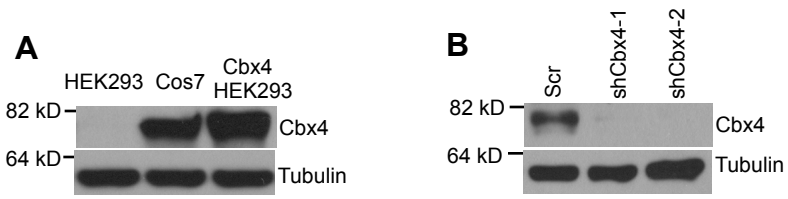

Figure S2, related to Figure 3. (A) Expression of endogenous Cbx4 protein in HEK293 cells and Cos7 cells. (B) Cbx4 protein level in Cos7 cells after lentiviral knockdown.

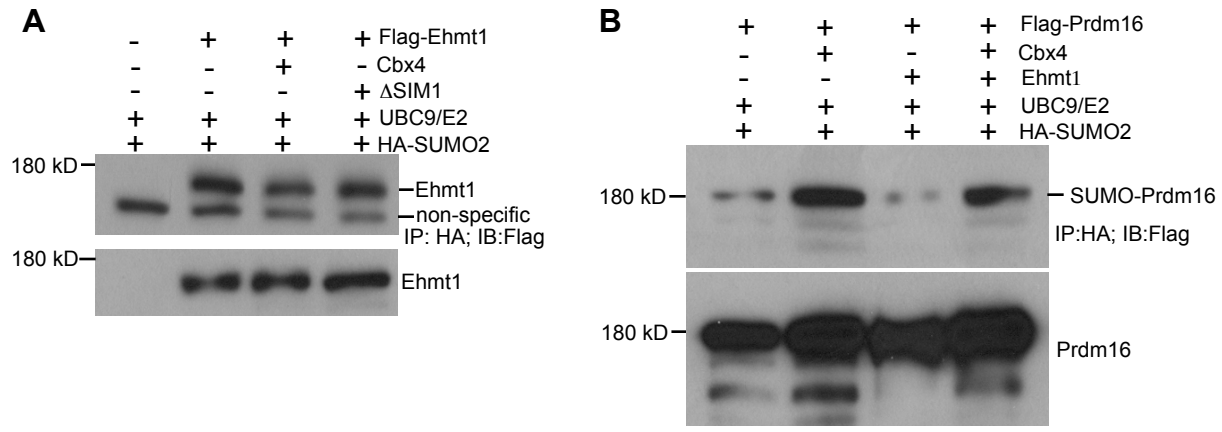

Figure S3. Related to Figure 3. Cbx4 does not sumoylate Ehmt1 (A) and Ehmt1 does not increase Cbx4 sumoylation activity (B). HEK293 cells were transfected with indicated plasmids and treated with MG132 for 16 hr before harvesting for immunoprecipitation.
(A) Sumoylation of Ehmt1. (B) Sumoylation of Prdm16.

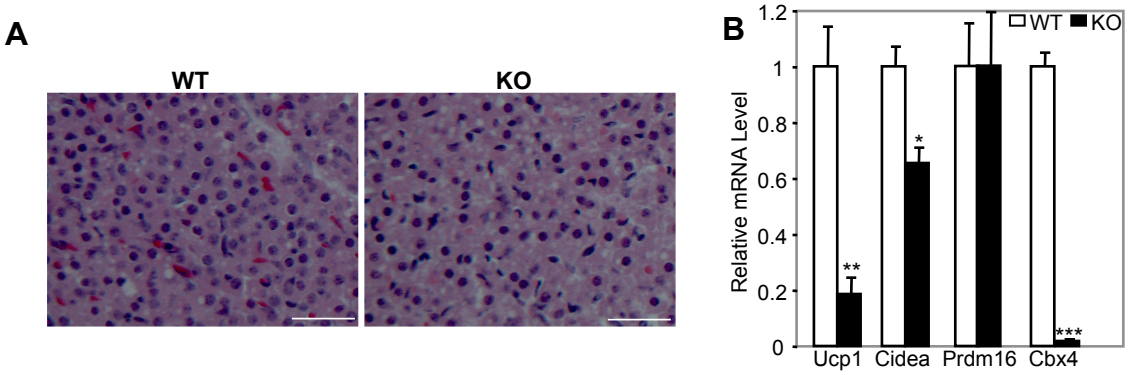

Figure S4, related to Figure 5. (A) H&E staining of BAT isolated from neonatal Cbx4 null mice. Shown are representative images of three mice per group. Scale bar=200 μm.
(B) Gene expression in BAT isolated from 18.5 Day embryos of Cbx4 null. Data represent mean ± SEM. *p<0.05,**p<0.01,***p<0.001.

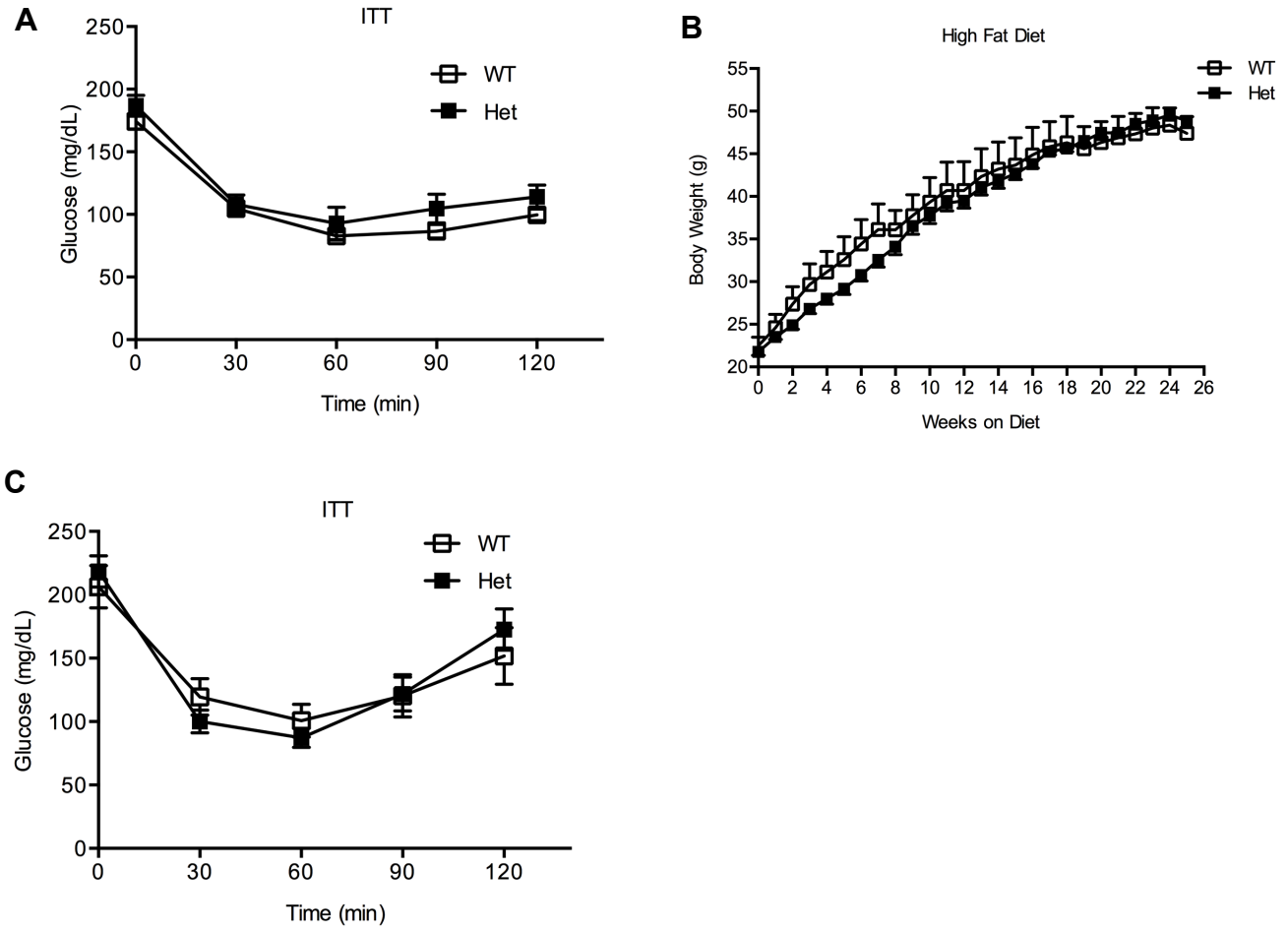

Figure S5, related to Figure 6. (A) Insulin tolerance test of 10-month-old male wild type and Cbx4 heterozygous mice (n=6-8 mice/group). (B) Body weights of male wild type and Cbx4 heterozygous mice fed a high fat diet (n=6 mice/group). (C) Insulin tolerance test of male wild type and Cbx4 heterozygous mice fed a high fat diet for 25 weeks (n=5-7 mice/group). Data represent mean ± SEM.

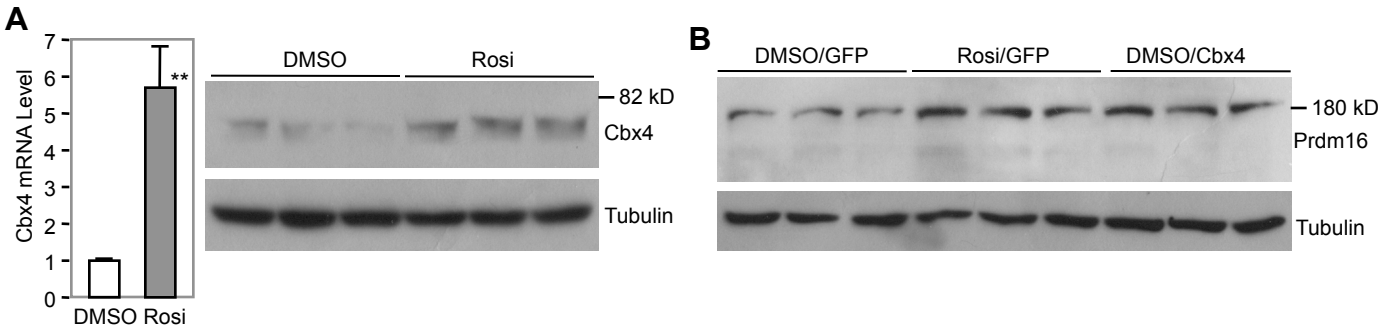

Figure S6, related to Figure 4. (A) Primary iWAT adipocytes were treated with Rosiglitazone (1 μM) during differentiation, and Cbx4 mRNA (n=4) and protein were measured. Data represent mean ± SEM. **p<0.01.

(B) Adipocytes were treated with Rosiglitazone or were infected with Cbx4 adenovirus, and Prdm16 protein was measured.